Journal of the Serbian Chemical Society
JSCS-info@shd.org.rs • www.shd.org.rs/JSCS
J. Serb. Chem. Soc. 77 (3) 259–277 (2012)
JSCS–4266
UDC 547.565.2–304.2+577.354:
547.53.024+547.861.3:539.196
Original scientific paper

Modeling key interactions between the second extracellular loop of the dopamine D2 receptor and arylpiperazine ligands

VLADIMIR ŠUKALOVIĆ[1*#], VUKIĆ ŠOŠKIĆ[2], DEANA ANDRIĆ[3], GORAN ROGLIĆ[3] and SLADJANA KOSTIĆ-RAJAČIĆ[1#]

[1]ICTM – Department of Chemistry, University of Belgrade, Njegoševa 12, 11000 Belgrade, Serbia, [2]ProteoSys AG, Carl Zeiss 51, 55129 Mainz, Germany and [3]Faculty of Chemistry, University of Belgrade, Studentski trg 12–16, 11000 Belgrade, Serbia

(Received 28 October 2011)

Abstract: Second extracellular loop (ecl2) of the dopamine (DA) D2 receptor is an essential part of the binding pocket of dopaminergic ligands. To form a part of the ligand-binding surface, it has to fold down into the transmembrane domain of the DA receptor. The current study describes the modeling of the D2 DA receptor ecl2 and its interactions with arylpiperazine ligands. In order to model the D2 DA receptor ecl2, several arylpiperazine ligands were used to propose a pharmacophore model. D2 DA receptor ecl2 model was built using Accelrys Discovery Studio. To test the proposed model, docking analysis was performed and key amino acid residues were determined. The proposed receptor–ligand interactions were rationalized and compared with measured binding affinities. It is shown that D2 DA receptor ecl2 significantly participates in the formation of the receptor–ligand complex through aromatic, hydrophobic and polar interaction. Considering them would benefit molecular modeling of G-protein-coupled receptors (GPCRs) and facilitate the design of novel active compounds.

Keywords: extracellular loop; dopamine; arylpiperazine; molecular modeling; GPRC.

INTRODUCTION

The catecholamine dopamine (DA) has been associated with many physiological functions such as fine movement coordination, cognition, emotion and memory by the mesocortical and mesolimbic reward systems.[1]

Alterations in dopaminergic function are involved in the pathogenesis of Parkinson's disease,[2] psychomotor diseases and schizophrenia.[3]

* Corresponding author. E-mail: v.sukalovic@hibcy.com
# Serbian Chemical Society member.
doi: 10.2298/JSC111028212S

The DA receptor system has been aggressively targeted for drug development for the treatment of psychiatric illnesses, neurodegeneration, drug abuse, and other therapeutic areas.[4,5] The DA receptors, belonging to the class of G-protein-coupled receptors (GPCRs), are found in both the peripheral and central nervous system (CNS).[3] The D2 DA receptor is a GPCR located on postsynaptic dopaminergic neurons that is heavily involved in reward-mediating mesocorticolimbic pathways. Signaling through D2 DA receptors governs physiological functions related to locomotion, hormone production, and drug abuse. D2 DA receptors are also known targets for antipsychotic drugs used to treat psychomotor diseases such as schizophrenia.[6] Although the biophysical and pharmacological properties of D2 DA receptors have been the subject of a number of studies,[7] many questions remain unresolved due to the lack of three-dimensional structures and other experimental limitations.

An enormous amount of work has been performed toward the development of various D2 DA receptor ligands. These efforts yielded a class of compounds known as dopaminergic arylpiperazine ligands.[8]

The pharmacophore of dopaminergic arylpiperazines has been well studied in experiments and molecular simulations.[9] Published results and 3D models explain to some extent the binding mechanism of arylpiperazine to the D2 DA receptor,[10–12] but still a complete understanding of the process is lacking, notably in the case of ligands that protrude from the canonical receptor binding site into the extracellular loop area. To obtain a better understanding of receptor–ligand interactions, a more precise model of the D2 DA receptor is required.

In this paper, focus will be centered on the extracellular loop area of the D2 DA receptor, particularly on the E2 loop segment. Considering that the crystal structures of D2 DA receptors are not available, *in silico* methods were used to gain further insight into the binding interactions between the extracellular loop area of D2 DA receptors and a new series of dopaminergic arylpiperazines.

EXPERIMENTAL

Ligand construction

The 3D structures of the ligands were generated using the Discovery Studio program.[12] Assuming physiological conditions, the basic aliphatic nitrogen atom of the piperazine was protonated. The geometry was optimized using the CHARMM force field applying the conjugate gradient method until the energy difference between successive cycles was below 0.0042 kJ mol^{-1}.

Pharmacophore model generation

The set of ligands used for pharmacophore generation consisted of the structures shown in Tables I and II with their dopamine D2 receptor binding affinities listed. The molecules were stored in a molecular database. This database was used as an input in the Discovery Studio pharmacophore protocol[12].

TABLE I. Arylpiperazine ligands showing moderate to high D2 affinity

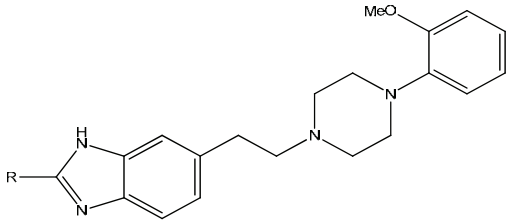

No.	R	K_i / nM
1[13]	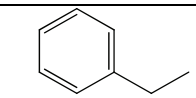	2.9
2[13]	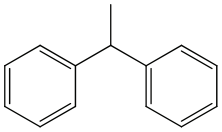	56.0
3[14]	CH_3SCH_2–	15.4
4[14]	CH_3SOCH_2–	24.8

The objective of the pharmacophore protocol is to generate all popular pharmacophore queries (with coverage *n*, typically 90 % or more of all active molecules) considering all possible discrete geometries with all possible combinations of input query expressions. The pharmacophore protocol operates on the 3D conformations of the molecules present in the input database. In the present study, the Conformations option in Pharmacophore protocol panel was set to BEST quality, wherein the rotatable bonds of each molecule were explored systematically to specific torsion angles from a collection of rules. The ring conformations were not searched; the chair conformation was assumed preferred as most of the docking runs finished with the ligands having the ring in the chair conformation.

Using these features for the determination of the minimal pharmacophore together with the enabled alignment of the aromatic ring atoms led to meaningful pharmacophore hypotheses. The pharmacophore protocol generated pharmacophores compatible with the minimal number of set features. Other parameter values in the pharmacophore protocol panel were kept at their default values. The results of the pharmacophore generation were written to an output database, which was analyzed further to visualize the appropriate pharmacophore hypothesis. The selection of the final hypothesis was based on an overall alignment score and the associated pharmacophore features.

Molecular modeling of D2 DA receptor extracellular loops

The starting point for molecular modeling was the currently valid loop-less dopamine D2 receptor model.[9] The Discovery Studio program package[12] was used to model the sequences of D2 DA receptor loops. Missing loops sequences were aligned with the D2 receptor sequence and this alignment was supplied along with the 3D coordinates of the existing model as an input to the program. A key determinant of the correct orientation of the extracellular loops is the constrain imposed by the position of the corresponding receptor helixes and a disulfide bond between the ecl2 and the top of the TM domain 3. The Discovery Studio loop refining implements protein loop modeling by satisfying these restraints while keeping the

existing part of the model fixed. This was followed by spatial constraints that were imposed to selected amino acid residues in order to satisfy the pharmacophore hypothesis. In order to obtain a relaxed conformation, the generated models were initially subjected to an energy minimization process using the conjugate gradient method for about 4000 iterations and to 2-ns isothermal, constant-volume MD simulation, with CHARMM all-hydrogen amino acid parameters in the Discovery Studio program running on a PC.[15] To assess the quality of the minimized models, Proteincheck[12] analysis was also undertaken. Initially, several possible models were constructed but the best possible model was considered the receptor "energy minima".

Docking analysis

Docking of the selected ligands as presented in Tables I–III was realized by simulated annealing using the LIBDOCK module from Discovery Studio. All ligands were docked as protonated, using the CHARMM force field. Amino acid residue charges were adjusted when needed. The protein-binding site was determined by combining results from experimental data and the Discovery Studio bind site analysis module.[12] Initial position of the ligand in the binding site was defined by keeping the protonated nitrogen on the ligand in close proximity to the Asp80 of the D2 receptor. After initial ligand placement, no further constraints were applied and the docking procedure based on Monte Carlo methodology was performed. Up to 100 structures were produced in every run and each finally optimized in order to remove steric interaction with a gradient limit of 0.0042 kJ mol^{-1} or 4000 optimization steps.

TABLE II. The arylpiperazine ligands used in the generation of the pharmacophore model and the docking analysis (marked +)

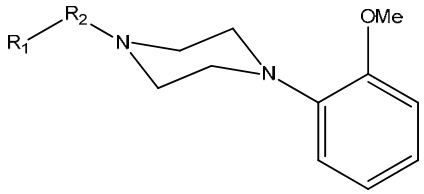

No.	R_1	R_2	K_i / nM
5[16]	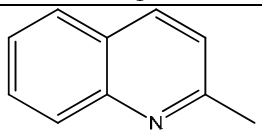	–CONH$(CH_2)_4$–	83±5
6[16]	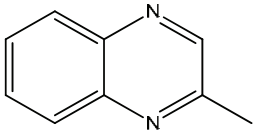	–CONH$(CH_2)_4$–	84±2
7+[16]	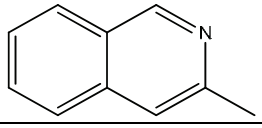	–CONH$(CH_2)_4$–	75±12

TABLE II. Continued

No.	R_1	R_2	K_i / nM
8+[16]	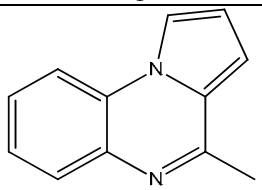	–CONH$(CH_2)_4$–	59±9
9[16]	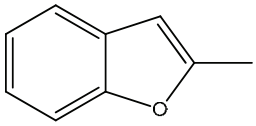	–CONH$(CH_2)_4$–	87±19
10[16]	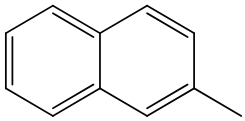	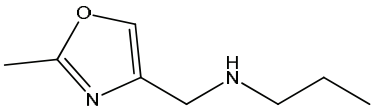	86±1
11[16]	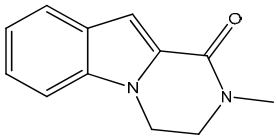	–$(CH_2)_4$–	45±7
12[17]	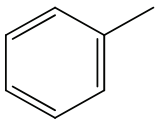	–CH=CH–CONH–$(CH_2)_4$–	13±1
13[17]	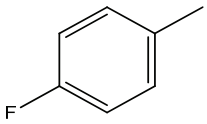	–CH=CH–CONH–$(CH_2)_4$–	20±1
14[17]	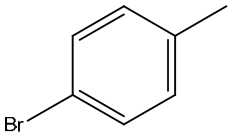	–CH=CH–CONH–$(CH_2)_4$–	23±1
15[17]	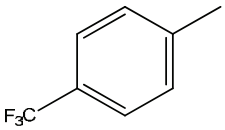	–CH=CH–CONH–$(CH_2)_4$–	37±6
16+[17]	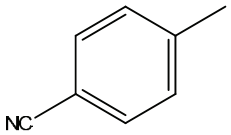	–CH=CH–CONH–$(CH_2)_4$–	10±0.7
17[17]	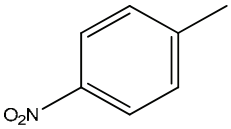	–CH=CH–CONH–$(CH_2)_4$–	14±3

TABLE II. Continued

No.	R_1	R_2	K_i / nM
18+[17]	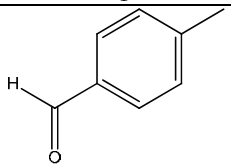	–CH=CH–CONH–$(CH_2)_4$–	11±2
19[17]	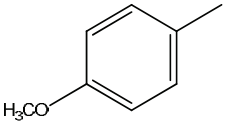	–CH=CH–CONH–$(CH_2)_4$–	12±1
20[17]	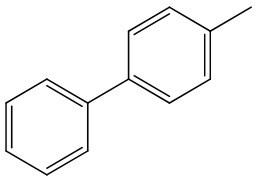	–CH=CH–CONH–$(CH_2)_4$–	37±15
21[17]	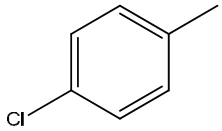	–CONH$(CH_2)_4$–	19±1
22[17]	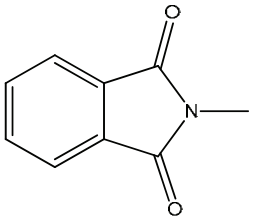	–$(CH_2)_4$–	50±6
23+[17]	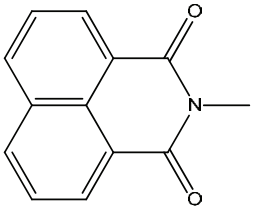	–$(CH_2)_4$–	40±3
24[18]	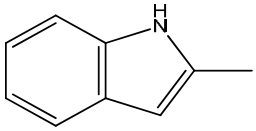	–CONH–$(CH_2)_4$–	37±6
17+[18]	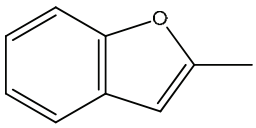	–CONH–$(CH_2)_4$–	36±4

TABLE II. Continued

No.	R_1	R_2	K_i / nM
18[18]	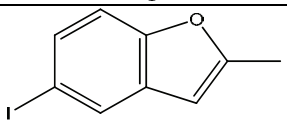	–CONH–$(CH_2)_4$–	77±17
19+[18]	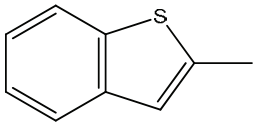	–CONH–$(CH_2)_4$–	21±2
28[18]	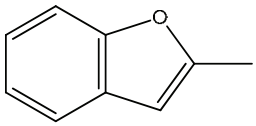	–CONH–CH_2CH=$CHCH_2$–	79±2
29[18]	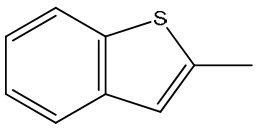	–CONH–CH_2CH=$CHCH_2$–	60±7
30[18]	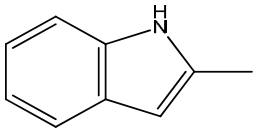	–CONH–CH_2CHOH–$(CH_2)_2$–	52±3
31[19]	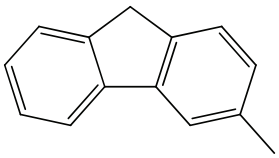	–CONH–$(CH_2)_4$–	55±5
32+[19]	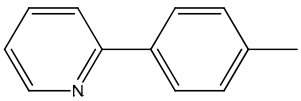	–CONH–$(CH_2)_4$–	28±6
33[19]	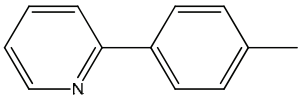	–CONH–CH_2CH=$CHCH_2$–	69±13
34+[19]	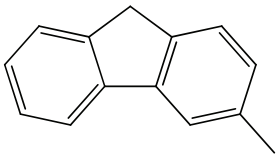	–CONH–CH_2CH=$CHCH_2$–	48±7
35[19]	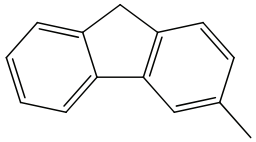	–CONH–CH_2CHOH–$(CH_2)_2$–	68±6

TABLE II. Continued

No.	R_1	R_2	K_i / nM
36+[20]	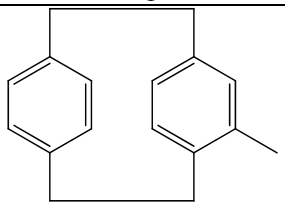	–CONH–$(CH_2)_4$–	15±1
37+[21]	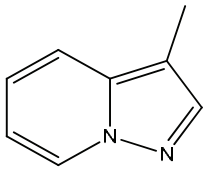	–CONH–$(CH_2)_3$–	11±1

TABLE III. Arylpiperazine ligands used in the testing of the receptor model

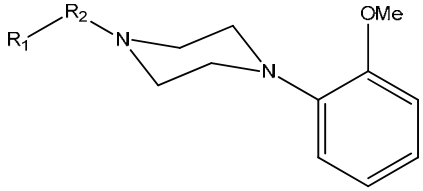

No.	R_1	R_2	K_i / nM
38[19]	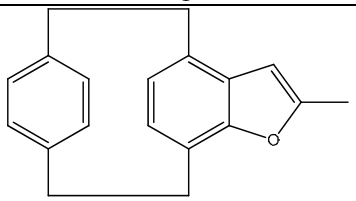	–CONH$(CH_2)_4$–	83±5
39[16]	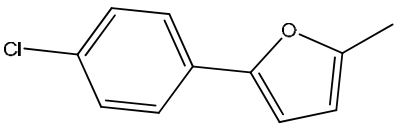	–CONH$(CH_2)_4$–	200±30
40[22]	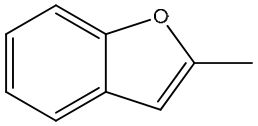	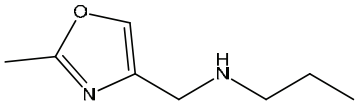	518±193

The obtained docked structures were examined, and those with the lowest total energy were further filtered to obtain docking structures with the best ligand fit. We selected structures based on the following criteria: lowest total energy of the complex, shortest salt bridge formed between Asp80 of the D2 receptor and the proton on nitrogen, chair conformation of arylpiperazine ring and the aryl part of the molecule positioned in the rear hydrophobic pocket of the receptor were selected. After the initial criterion was satisfied, the second step was examination of different interactions that could be formed between the receptor and ligand (hyd-

rogen bonds, aromatic–aromatic interactions, *etc*.). In this way, the best possible docking structures were selected. Structures were visualized using DS Visualise v2.5.1[23] and the obtained images were rendered using PovRay Raytracer v3.6.[24]

RESULTS AND DISCUSSION

The currently used loop-less D2 DA receptor model could not explain the binding affinities for a number of synthesized arylpiperazine ligands (Table I). Docking analysis suggested that these ligands are not able to fit into the existing binding site[9] due to their size, and that they protruded into the extracellular loop (ecl) area of the D2 DA receptor. The importance of the ecls for accommodating high molecular weight GPCR ligands (peptides and proteins) is widely accepted.[25] Recent studies indicate the same could be true for low molecular weight ligands.[22,26,27]

These findings emphasized that a new D2 model that includes the loops, should be constructed. In this study the focus was on the modeling of the extracellular loops as they border the receptor binding site and could interact with ligand molecules.[28]

Receptor loop modeling is a challenging task because, in contrast to the alpha helix or beta sheet, they do not fit into the defined 3D template and a careful decision has to be made on how to differentiate between a myriad of possible conformations.

Initial attempts to model the D2 receptor with loops *in silico*, using different existing templates, failed to produce a viable model. Construction of the ecls should be realized with care and guided by receptor-specific experimental data, rather than being performed in a high-throughput fashion and derived directly from the known crystal structure.[29]

In order to solve this problem, computational methods, pharmacophore model generation and docking analysis, together with experimental results, were applied in this study. Apart from general ecl2 modeling, the aim of this study was to discover the ecl2 amino acid residues responsible for D2 DA receptor–ligand interactions. The pharmacophore model hypothesis predicts the type of receptor––ligand interactions, thus ecl2 was modeled in a way to facilitate such interactions, and docking analysis was employed to confirm that these interactions are *de facto* possible.

Pharmacophore model generation requires a considerable ligand database, which was obtained from available literature sources.

To facilitate the search, the molecular structure of the arylpiperazine ligands was divided into three distinct substructure motives: tail (arylpiperazine substructure), flexible linker and head part (usually the bulky aromatic group, see Fig. 1). The tail part of the ligand was kept fixed, while the linker and head part were subjected to variations in length and size. The tail part was fixed to 1-(2-methoxyphenyl)piperazine since the interaction of this structural motive with the D2

DA receptor is well investigated.[10] The length of the linker is crucial for the receptor–ligand interaction, since it positions the head of the ligand against the amino acid residues located in the extracellular loops of the receptor, and was therefore allowed to vary. In addition, differences in size, shape and functionality of the head were tolerated, allowing investigation of the influence of these molecular diversities on the ligand binding affinity. More than 80 ligands were considered of which, 33 were selected for further investigation. Only ligands with a moderate to high affinity (K_i under 100 nM) were taken into consideration.

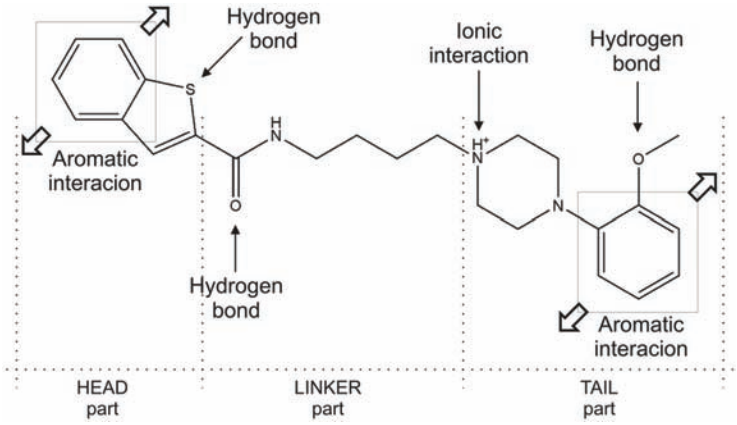

Fig. 1. Schematic presentation of the proposed key interactions, generated by the pharmacophore hypothesis.

Pharmacophore model generation was performed using Discovery Studio, as described. In total, 33 ligands were used to generate the pharmacophore model hypothesis. The obtained results are shown in Figs. 1 and 2. The pharmacophore model hypothesis suggests salt bridge formation between the protonated piperazine nitrogen atom and the receptor, one or more aromatic interactions at the tail part of the ligand, together with a hydrogen bond between the oxygen atom of the methoxy group and the receptor. In the linker part, there is the possibility of hydrogen bond formation, while in the head part of the ligand, one or more interactions were expected. These interactions could be of an aromatic nature or a hydrogen bond, depending of the chemical structure of the head of the ligand.

Docking studies of these bulky ligands performed with the loop-less D2 DA receptor model could not explain the high affinities obtained in the binding studies. Therefore, it was hypothesized that some additional interaction with the out--of-membrane receptor domain is involved. Molecular modeling that took into consideration interactions with ecl2 gave the best results. The ligands that can form additional aromatic type interaction or hydrogen bond in the head part can do so exclusively with amino acid residues located in the ecl2 region of the D2

DA receptor. Other proposed ligand–receptor interactions, such as the salt bridge formed between ASP80 and the protonated piperazine nitrogen, hydrophobic interactions between PHE178, TRP182 and TYR212 and arylpiperazine, and hydrogen bond formation between the 2-methoxy group oxygen and TYR212, are located in the transmembrane domain of the receptor molecule and are described in an earlier publication.[9]

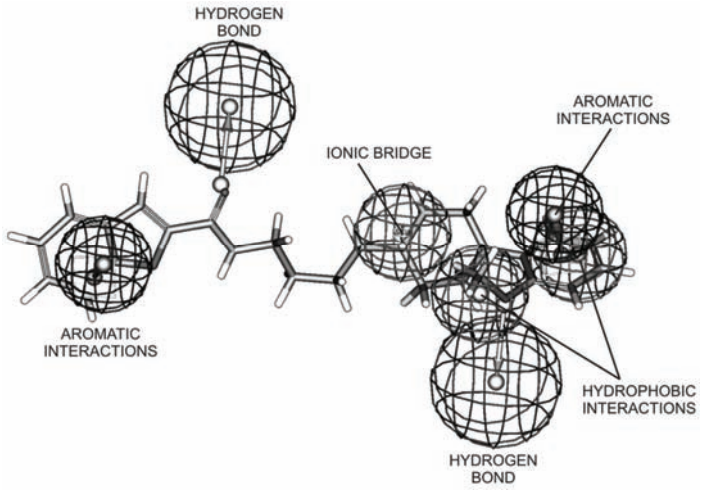

Fig. 2. Proposed pharmacophore hypothesis mapped on ligand **9**. Proposed key interactions are shown as vectors and spheres, depicting the direction and space where a particular interaction is expected.

Modeling of the ecl2 is described in the experimental part; particular attention was given to the orientation of the hydrophobic amino acid residues as good candidates to form aromatic interactions with ligands.

The generated DA D2 receptor models with extracellular loops were tested using docking analysis until a satisfactory model that could explain the binding and activities of the selected ligands was obtained.

In total, 11 literature ligands with activities ranging from 10 to 75 nM were selected for the docking analysis (Table II). It was decided to use ligands that had a significant affinity towards the D2 DA receptor while taking into account the structural diversity that could account for the proposed aromatic interactions and hydrogen bond formation with the ecl2 of the D2 DA receptor.

Preliminary ligand docking was performed to allow the ligand to position itself inside the binding site. After a satisfactory ligand orientation had been obtained (salt bridge formation between ASP80 and the protonated ligand nitrogen atom, aryl moiety positioned inside the hydrophobic pocket formed by PHE178, TRP182 and TYR212, one or more hydrogen bonds formed with SER149 and/or SER122), fixed atom constraints were applied on the ligand and receptor amino

acids backbone, excluding those in the ecls that were allowed to move freely. An additional docking run was executed whereby optimal positioning of the ecls amino acid residues was allowed. Finally, molecular dynamics calculations followed by energy minimization were performed to remove any steric interactions. The obtained results are shown in Figs. 3–6. Thus, it is shown that the selected ligands can bind into proposed D2 DA receptor model and form interactions with the amino acid residues of the ecl2 loop, as required by the pharmacophore hypothesis, while simultaneously concurring with recent findings (Fig. 3).[12,28]

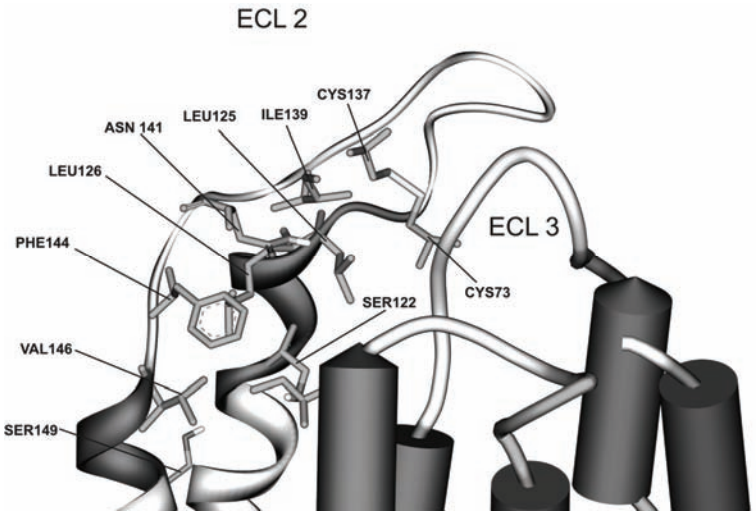

Fig. 3. Generated model of ecl2. Key amino acid residues responsible for interactions with the investigated ligands obtained by docking analysis are shown together with the conserved disulfide bond between ecl2 and ecl3.

All the investigated ligands bind in a similar manner. The main features of the docked complexes are short salt bridges between the protonated nitrogen of the piperazine ligand and ASP80 and the number of interactions formed by the aryl tail section and the corresponding amino acids (PHE178, TRP182 and TYR212).

Ligand **36** is the bulkiest ligand, with a high receptor affinity (Fig. 4). Its large hydrophobic head must be docked into the appropriate hydrophobic receptor pocket that is formed by the amino acid residues LEU125, LEU126, ILE139, VAL146, PHE144, HIS189 and ILE190. The head of the ligand can form a number of hydrophobic interactions with the listed amino acid residues. Special attention should be given to PHE144 and HIS189, as they are in a range that could lead to the formation of edge-to-face (etf) interactions. These interactions together with the hydrogen bond formed with SER122 are responsible for the high ligand affinity.

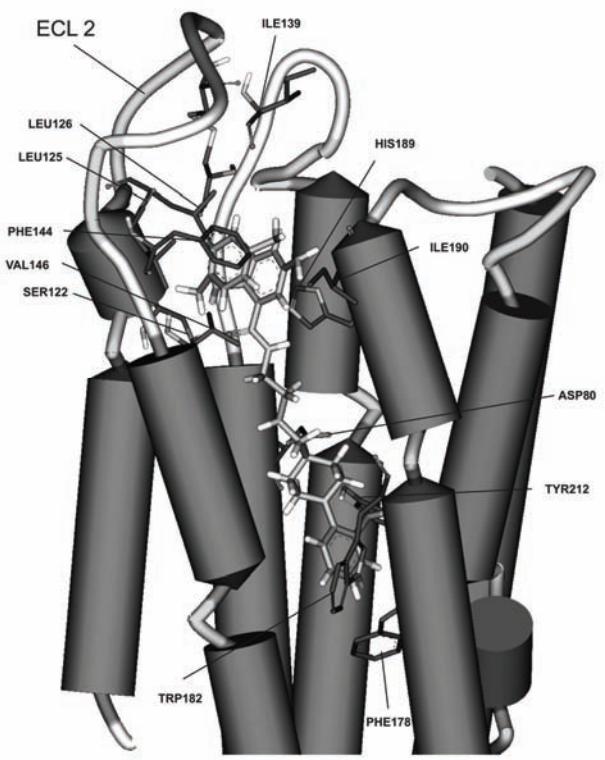

Fig. 4. Docking results for ligand **36**. Only key amino acid residues are shown for clarity.

Ligands that have large hydrophobic groups in the head part (ligands **7**, **8**, **23**, **25**, **32**, **34** and **37**) bind to the hydrophobic pocket that is formed in part by ecl2 (Fig. 5). This is the same pocket formed by PHE144, LEU125, ILE139, LEU126, VAL146 and ILE190, as in case of ligand **36**. Docking analysis shows possible interactions formed by PHE144 (edge-to-face) and HIS189 on TM6 (NH···Pi or CH···Pi) interactions with the ligand.

Ligand **16** (Fig. 5) and ligands **13**–**15** and **17**–**19** are somewhat different as their head part contains groups capable of forming polar interactions or hydrogen bonds. In the case of these ligands, in addition to the already listed interactions, polar interactions with ASN141 in ecl2 could account for their activity.

All ligands from Table II form one or more interactions with ecl2, based on their structure, and these interactions are responsible for their activity. For example, ligands **12**, **13**, **24**, **36**, **38**–**41** form aromatic interactions with hydrophobic amino acid residues. These interactions may include edge-to-face interactions with PHE144 and HIS189. Ligands **16**–**23** can form either hydrogen bonds or polar interactions with ASN141. Ligands **4**–**14**, **26**–**35** and **42** can benefit from listed aromatic interactions and hydrogen bond with SER122.

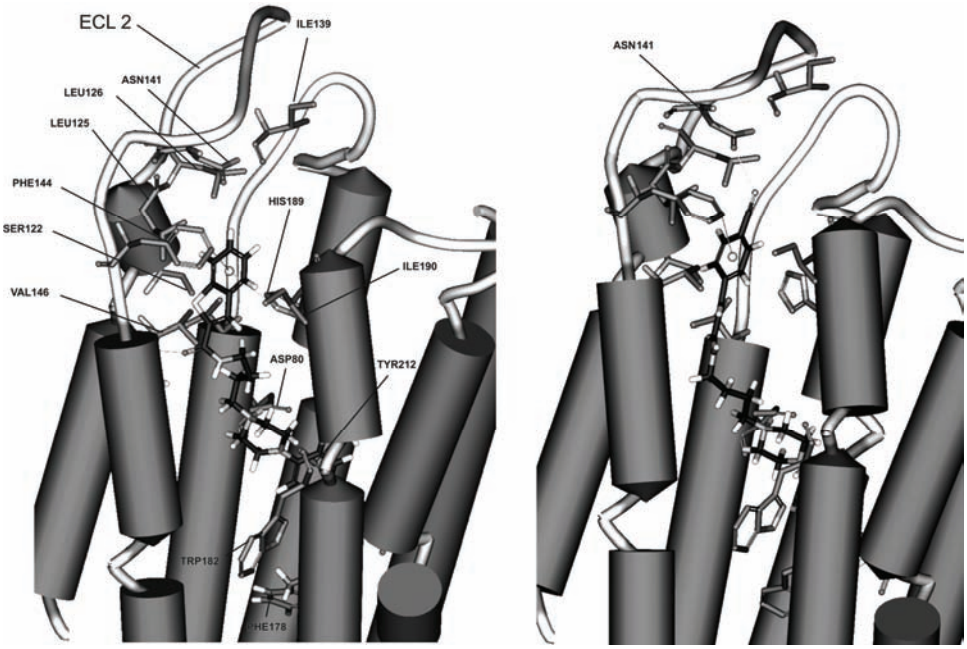

Fig. 5. Ligands **27** (left) and **16** (right) docked into the D2 receptor. Only key amino acid residues are shown for clarity.

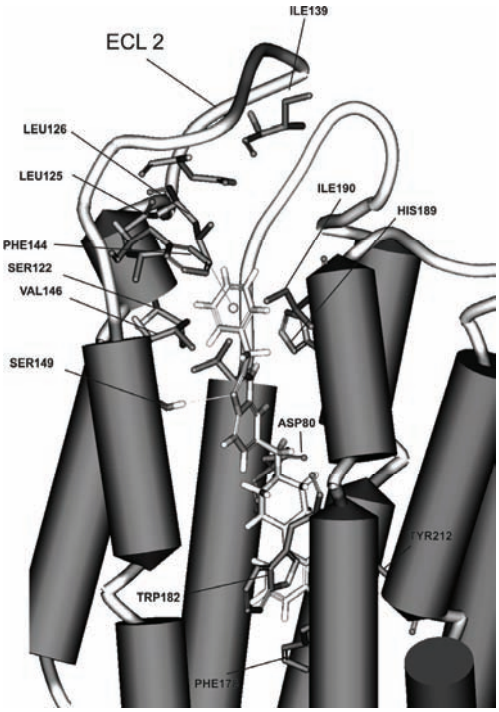

Fig. 6. Ligand **1** docked into the proposed D2 model. Possible interactions with PHE144 and SER 149 are marked as lines.

The final test of the model was its ability to discriminate high affinity *versus* low affinity ligands. The test was performed on compounds homologous to the active ligands (Table II) but with significantly lower D2 DA receptor affinity. Chemical structures alongside the affinity data of these compounds are presented in Table III.

The results of docking analysis are shown in Fig. 7. Ligand **38** is similar to **36**, yet its binding affinity is 10-fold lower. The ligand cannot optimally fit into the proposed pocket, formed by elc2 amino acid residues, as multiple bump interactions with SER122 and HIS189 are observed (Fig. 7, left), furthermore due to different ligand orientation hydrogen bound with SER122 is lacking.

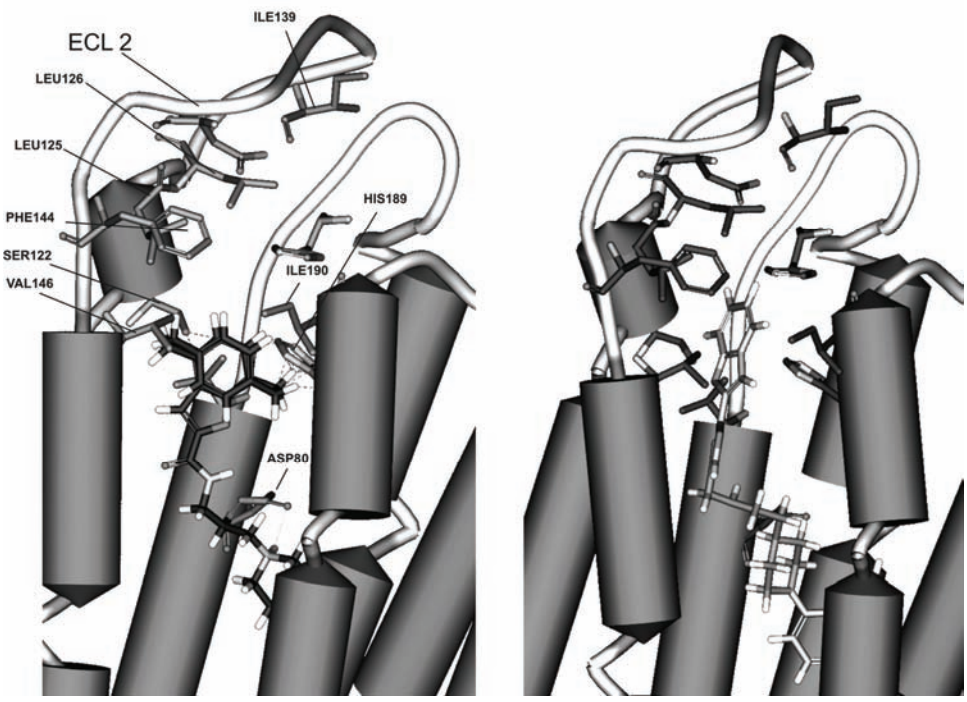

Fig. 7. Docking results for the low affinity arylpiperazine ligands **38** (left) and **40** (right). Only key amino acid residues are shown. Bump interactions are marked as dashed lines.

Ligand **40** is similar to ligand **10**. The increase in overall length of ligand **40** is a key factor for its ten-fold decrease in affinity. Being both long and rigid, ligand **40** suffers from unfavorable steric interactions with amino acid residues in the receptor ecl2. Due to its inability to fit into the binding site, all the observed key interactions have longer distances. Most notably, the salt bridge with ASP80 is elongated by 1 Å, and the hydrogen bonds with SER122 and SER149 are con-

siderably longer (3.57 and 3.92 Å compared to 2.47 and 2.98 Å in ligand **10**, Fig. 7, right).

Similar factors can explain the seven-fold decrease in affinity of **39** *vs*. **21**. In the case of ligand **39**, the introduction of the furan ring into the head segment leads to a loss in binding affinity, due to steric interaction between the chlorine atom and ASN141. This steric interaction pushes the ligand down into the binding site, making the key interactions with ASP80 and SER122 longer by 1 Å (Fig. 8).

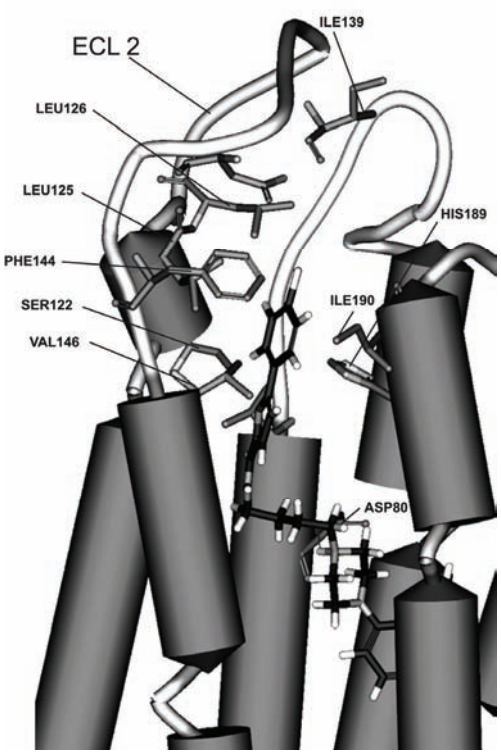

Fig. 8. Docking result for the low affinity arylpiperazine ligand **39**. Only key amino acid residues are shown.

Finally, the proposed D2 DA receptor model was used to explain the binding affinities of the ligands shown in Table I. Docking results showed that ligands **1** and **2** forms multiple aromatic interactions with PHE144, LEU125, LEU126 and VAL146 (Fig. 6). Ligands **3** and **4**, which cannot form aromatic interactions, still benefit from hydrogen bonds formation or polar interactions with ASN141 in ecl2.

CONCLUSION

The primary aim of the current study was to provide a new D2 DA receptor model that includes ecls that is capable of explaining existing experimentally obtained affinity data for bulky arylpiperazine type ligands.

Modeling ecls residues *in silico* is highly speculative as they are located in the part of the molecule that cannot be directly derived from the existing structural templates. Although the recent publishing of the crystal structure of the D3 DA receptor[17] is a significant step forward, it was decided to employ the existing, experimentally proved D2 DA receptor model, which was made by combining *in silico* methods and experimental data and proved by experimental results.[9–11] Still, the exact structure of the D2 DA receptor remains unknown and, therefore, every model that can explain experimental data should be considered. The model described in this study can explain the DA receptor binding properties of arylpiperazine classes of ligands; hence, it could be of great value for virtual screening studies.

The employed approach in modeling ecls was twofold. First, a pharmacophore model was constructed using a number of different ligands, having a common arylpiperazine moiety. This model indicated to a number of possible interactions between a ligand and the receptor, including interactions in the ecl2 part. Based on these assumptions, the ecls were modeled. Then, docking analysis was performed to position the ligand inside the receptor-binding site, until all known interactions were established. The ecl2 residues were then adjusted to form other interactions predicted by the pharmacophore model. Further energy minimization and molecular dynamics were used to refine the obtained results.

During the modeling process, a number of key amino acid residues located in the ecl2 that could form interactions with ligands were observed. These interactions, which lead to high ligand affinity, included aromatic interactions with PHE144, LEU125, LEU126, VAL146 and ILE190 and polar interactions with ASN141. Aromatic interactions are most likely edge-to-face type with PHE144 or CH···Pi (or NH···Pi) interactions with HIS189. Polar interaction with ASN135 could also be responsible for the high binding affinity of ligands with the corresponding functional groups. The size of the ligand is important. Short ligands do not benefit from interactions with ecl2, while long ones suffer from steric interactions with amino acid residues in the loop. The head part of the ligand should have at least one aromatic ring, but systems with two or more aromatic rings are well tolerated unless the maximum allowed length of the ligand is attained. High affinity could be achieved by aromatic interactions alone, or together with polar interactions. Ligands with halogen atoms or polar groups have affinities comparable with those of their aromatic analogues. The linker part of the ligand should be as flexible as possible, since its primary function is to allow the optimum positioning of the head part into the space formed by the ecl2.

For the sake of verification of the proposed D2 DA receptor model, further work on the target-driven synthesis of new ligands that can distinguish between the proposed molecular interactions are necessary. The final goal is to obtain a

workable D2 DA receptor model that will facilitate the design of new specific dopaminergic drugs.

Acknowledgement. This research was part of project 172032 funded by the Ministry of Education and Science of the Republic of Serbia.

И З В О Д

МОДЕЛОВАЊЕ КЉУЧНИХ ИНТЕРАКЦИЈА ИЗМЕЂУ ДРУГЕ ЕКСТРАЦЕЛУЛАРНЕ ПЕТЉЕ ДОПАМИНСКОГ D2 РЕЦЕПТОРА И АРИЛПИПЕРАЗИНА КАО ЛИГАНАДА

ВЛАДИМИР ШУКАЛОВИЋ[1], ВУКИЋ ШОШКИЋ[2], ДЕАНА АНДРИЋ[3], ГОРАН РОГЛИЋ[3] и СЛАЂАНА КОСТИЋ-РАЈАЧИЋ[1]

[1]ИХТМ – Центар за хемију, Универзитет у Београду, Његошева 12, 11000 Београд, [2]ProteoSys AG, Carl Zeiss 51, 55129 Mainz, Germany и [3]Хемијски факултет, Универзитет у Београду, Студентски трг 12–16, 11000 Београд

Друга екстрацелуларна петља допаминског D2 рецептора је есенцијални део везивног места рецептора. Да би се дефинисала горња страна везивног места, она мора да се савије надоле, и оријентише ка трансмембранском домену рецептора. У овом раду описан је процес моделовања друге екстрацелуларне петље допаминског D2 рецептора и њене интеракције са арилпиперазинским лигандима. За моделовање је коришћен *Accelrys Discovery Studio* пакет програма. Предложени модел је тестиран докинг анализом литературно доступних лиганада и поређењем добијених резултата са њиховим афинитетом везивања за D2 рецептор. Одређени су амино-киселински остаци који ступају у интеракције са лигандима. Кључне интеракције су дефинисане и упоређене са афинитетима лиганада према рецептору како би се предложеним моделом објасниле разлике у експерименталним резултатима. Наша истраживања су показала да друга екстрацелуларна петља допаминског D2 рецептора може ступати у различите интеракције са арилпиперазинским лигандима које између осталих укључују хидрофобне, ароматичне интеракције али и водоничне везе. Ова сазнања, у комбинацији са предложеним моделом D2 рецептора, који укључује екстрацелуларне петље, могу бити од велике користи приликом будућег дизајна нових допаминергичких лиганада.

(Примљено 28. октобра 2011)

REFERENCES

1. C. Missale, S. R. Nash, S. W. Robinson, M. Jaber, M. G. Caron, *Physiol. Rev*. **78** (1998) 189
2. J. Lotharius, P. Brundin, *Nat. Rev. Neurosci*. **3** (2002) 932
3. S. Kapur, D. Mamo, *Prog. Neuropsychopharmacol. Biol. Psychiatry* **27** (2003) 1081
4. G. Emilien, J. M. Maloteaux, M. Geurts, K. Hoogenberg, S. Cragg, *Pharmacol. Ther.* **84** (1999) 133
5. E. P. Noble, *Am. J. Med. Genet., B* **116** (2003) 103
6. S. L. Payne, A. M. Johansson, P. G. Strange, *J. Neurochem*. **82** (2002) 1106
7. J. A. Javitch, D. Fu, J. Chen, A. Karlin, *Neuron* **14** (1995) 825
8. A. Zhang, J. L. Neumeyer, R. J. Baldessarini, *Chem. Rev.* **107** (2007) 274
9. V. Sukalovic, D. Andric, G. Roglic, S. Kostic-Rajacic, A. Schrattenholz, V. Soskic, *Eur. J. Med. Chem*. **40** (2005) 481
10. V. Sukalovic, M. Zlatovic, D. Andric, G. Roglic, S. Kostic-Rajacic, V. Soskic, *Arzneimittelforschung* **55** (2005) 145

11. V. Sukalovic, M. Zlatovic, D. Andric, G. Roglic, S. Kostic-Rajaccic, V. Soskic, *Arch. Pharm. (Weinheim)* **337** (2004) 502
12. Accelrys Software Inc., *Discovery Studio Modeling Environment, Release 2.5*, San Diego, CA, 2009
13. S. Kostic-Rajacic, V. Soskic, J. Joksimovic, *Arch. Pharm. (Weinheim)* **331** (1998) 22
14. S. Kostic-Rajacic, V. Soskic, J. Joksimovic, *Pharmazie* **53** (1998) 438
15. Intel Quad-Core CPU 2.4 GHz, 4 GB Ram, ATI Radeon 4570 HD Graphics
16. G. Campiani, S. Butini, F. Trotta, C. Fattorusso, B. Catalanotti, F. Aiello, S. Gemma, V. Nacci, E. Novellino, J. A. Stark, A. Cagnotto, E. Fumagalli, F. Carnovali, L. Cervo, T. Mennini, *J. Med. Chem*. **46** (2003) 3822
17. A. Hackling, R. Ghosh, S. Perachon, A. Mann, H. D. Holtje, C. G. Wermuth, J. C. Schwartz, W. Sippl, P. Sokoloff, H. Stark, *J. Med. Chem.* **46** (2003) 3883
18. A. H. Newman, P. Grundt, G. Cyriac, J. R. Deschamps, M. Taylor, R. Kumar, D. Ho, R. R. Luedtke, *J. Med. Chem*. **52** (2009) 2559
19. P. Grundt, E. E. Carlson, J. Cao, C. J. Bennett, E. McElveen, M. Taylor, R. R. Luedtke, A. H. Newman, *J. Med. Chem*. **48** (2005) 839
20. K. Schlotter, F. Boeckler, H. Hubner, P. Gmeiner, *J. Med. Chem*. **49** (2006) 3628
21. K. Ehrlich, A. Gotz, S. Bollinger, N. Tschammer, L. Bettinetti, S. Harterich, H. Hubner, H. Lanig, P. Gmeiner, *J. Med. Chem*. **52** (2009) 4923
22. E. Y. Chien, W. Liu, Q. Zhao, V. Katritch, G. W. Han, M. A. Hanson, L. Shi, A. H. Newman, J. A. Javitch, V. Cherezov, R. C. Stevens, *Science* **330** (2010) 1091
23. Discovery Studio Visualiser 2.5.1, Accelrys Software Inc., *Discovery Studio Modeling Environment, Release 2.5*, San Diego: Accelrys Software Inc., 2009
24. Pov-Ray *The Persistence of Vision Ray-Tracer, version 3.6*, 2003–2011, http:// //www.povray.org/ (Accessed Jun 12, 2011)
25. T. H. Ji, M. Grossmann, I. Ji, *J. Biol. Chem*. **273** (1998) 17299
26. J. S. Surgand, J. Rodrigo, E. Kellenberger, D. Rognan, *Proteins* **62** (2006) 509
27. J. L. Baneres, D. Mesnier, A. Martin, L. Joubert, A. Dumuis, J. Bockaert, *J. Biol. Chem.* **280** (2005) 20253
28. L. Shi, J. A. Javitch, *Proc. Natl. Acad. Sci. USA* **101** (2004) 440
29. C. de Graaf, N. Foata, O. Engkvist, D. Rognan, *Proteins* **71** (2008) 599.